








DMD-Unmanaged Long-Haul SDM Transmission Over 2500-km 12-Core \times 3-Mode MC-FMF and 6300-km 3-Mode FMF Employing Intermodal Interference Canceling Technique

Kohki Shibahara , Member, IEEE, Takayuki Mizuno , Senior Member, IEEE, Member, OSA, Doohwan Lee, Yutaka Miyamoto, Member, IEEE, Hirotaka Ono , Senior Member, IEEE, Kazuhide Nakajima , Member, IEEE, Member, OSA, Yoshimichi Amma , Katsuhiro Takenaga , and Kunimasa Saitoh , Member, IEEE, Member, OSA

(Post-Deadline Paper)

I. INTRODUCTION

Abstract—We demonstrate differential mode delay (DMD) unmanaged 2500-km 12-core \times 3-mode multicore few-mode fiber (MC-FMF) and 6300-km 3-mode FMF transmission. Mode-division multiplexed signals exhibit different transmission behavior depending on excited spatial modes in the presence of mode-relevant physical phenomena including DMD and mode-dependent loss (MDL). In weakly coupled FMF transmission over long distance where overall DMD and MDL grow almost linearly with fiber length, these phenomena restrict achievable information capacity and/or transmission reach. This paper presents a newly developed transmission scheme and a multiple-input multiple-output (MIMO) signal processing technique that are designed for achieving long-haul FMF transmission. Permutating spatial channels cyclically at each span induced quasi-strongly coupled transmission regime and hence significantly suppressed DMD-induced pulse broadening. Layered MIMO signal processing comprising multiple stages performing successive signal detection and intermodal interference canceling mitigated MDL impact with more than 2-dB Q-factor improvement. The combined use of these techniques enabled us to achieve the first-ever transoceanic-class long-haul FMF transmission.

Index Terms—Differential mode delay (DMD), mode dependent loss (MDL), MIMO equalization, space division multiplexing (SDM), successive interference cancellation (SIC).

Manuscript received June 29, 2018; revised September 17, 2018 and October 16, 2018; accepted October 17, 2018. Date of publication October 22, 2018; date of current version February 1, 2019. (Corresponding author: Kohki Shibahara.)

K. Shibahara, T. Mizuno, D. Lee, and Y. Miyamoto are with the NTT Network Innovation Laboratories, NTT Corporation, Kanagawa 239-0847, Japan (e-mail: shibahara.kouki@lab.ntt.co.jp; mizuno.takayuki@lab.ntt.co.jp; lee.doohwan@lab.ntt.co.jp; miyamoto.yutaka@lab.ntt.co.jp).

H. Ono is with the NTT Device Technology Laboratories, NTT Corporation, Atsugi 243-0198, Japan (e-mail: ono.hirotaka@lab.ntt.co.jp).

K. Nakajima is with the NTT Access Network Service Systems Laboratories, NTT Corporation, Tsukuba 305-0805, Japan (e-mail: nakajima.kazuhide@lab.ntt.co.jp).

Y. Amma, and K. Takenaga are with the Advanced Technology Laboratory, Fujikura Ltd., Sakura 285-8550, Japan (e-mail: yoshimichi.amma@jp.fujikura.com; katsuhiro.takenaga@jp.fujikura.com).

K. Saitoh is with the Hokkaido University, Sapporo 060-0814, Japan (e-mail: ksaitoh@ist.hokudai.ac.jp).

Color versions of one or more of the figures in this paper are available online at <http://ieeexplore.ieee.org>.

Digital Object Identifier 10.1109/JLT.2018.2877213

WITH the advent of space division multiplexing (SDM) technologies that transmit multiple channels utilizing spatial aggregation over multicore (MC) and/or fewmode fibers (FMFs) [1], the high potential of fiber capacity enhancement offered by SDM systems has been demonstrated by several high-capacity and/or long-haul SDM transmission experiments [2]–[8]. Employing spatial channels in MC-FMFs and FMFs as parallel waveguides has been an attractive approach to fully exploit spatial degrees of freedom of SDM fibers. Although over the past few years several long-haul FMF transmission experiments were successfully demonstrated with transmission distance up to 3500 km [9], there still remain many challenging issues to overcome in developing the future SDM systems. Inherent physical phenomena characterizing a FMF transmission line include differential mode delay (DMD) and mode dependent loss (MDL). In weakly-coupled FMF transmission where low energy exchange between different mode groups is stimulated during optical signal propagation, almost linear accumulation of overall DMD and MDL is observed with increased transmission distance [6], [10], [11]. This imposes negative impacts on achievable information capacity and multiple-input multiple-output (MIMO) signal detection processing. In particular, DMD induces pulse broadening for mode-division-multiplexed (MDM) signals, resulting in enhanced equalizer memory length (EML) as large as that corresponding to a thousand equalizer taps in receiver-side MIMO signal detection [12]–[14]. In the presence of a large MDL, the widely-used conventional linear MIMO equalizer suffers from residual intermodal crosstalk due to a non-unitary channel property. Consequently, these phenomena still remain as dominant barriers to extending FMF transmission reach. One of the approaches to combat DMD is DMD management DMD along transmission lines by concatenating positive/negative DMD FMFs [15], [16]. Alternatively, a strongly-coupled regime generally driven in coupled-core MC transmission fibers would be beneficial to statistically reduce

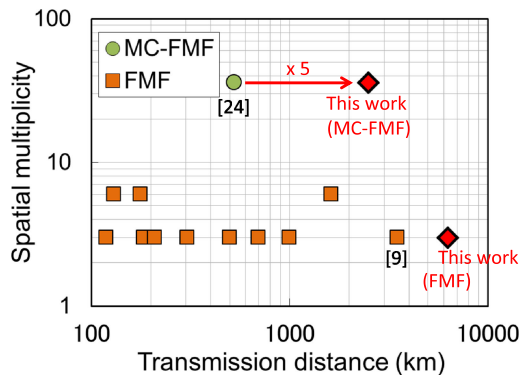


Fig. 1. SDM transmission distance vs. spatial multiplicity.

DMD and MDL impacts [11], [17]. In FMF transmissions, introducing intentional intermodal coupling may also provide advantages by employing mode scramblers comprising a mode multiplexer/demultiplexer pair [18], [19] or long-period fiber gratings [20]–[22]. With respect to future deployable terrestrial SDM systems, a DMD-unmanagement property is one of the key topics from the perspective of system design and operation.

In this paper, we extend the work presented in [8] with more detailed discussion where we demonstrate record-long wavelength division multiplexed (WDM) SDM transmission experiments over FMFs with transmission reach exceeding 2500 km for a 12-core \times 3-mode MC-FMF and 6300 km for a single-core FMF. Quasi-strongly-coupled FMF-based transmission lines were realized that helped to achieve DMD-unmanaged long-haul FMF transmission. The transmission strategy described in this paper, which we call cyclic mode permutation (CMP), cyclically shifts spatial mode signals every span as a means of inducing a strong intermodal coupling process. We also applied the intermodal interference cancelling technique proposed in our previous work [23] to long-haul FMF transmission as a means to extend transmission reach of MDM signal propagation in the presence of a large MDL. The achieved transmission reach of 2500 km over MC-FMF corresponds to a five-fold increase in transmission reach relative to that reported in previous work [24]. Furthermore, the 6300 km reach over FMF is the first-ever demonstration of ultra-long-haul transoceanic-class transmission employing FMFs.

The rest of this paper is organized as follows: Section II provides detailed descriptions of the newly-developed techniques that significantly contributed to the extended FMF transmission reach extension achieved. Then Section III describes an experimental setup that was designed to achieve reliable long-haul MDM signal transmission over FMFs. In Section IV, transmission performance enhancement attained with the proposed techniques is experimentally explored, followed by a demonstration of the long-distance transmission results. Finally, Section V concludes this paper with a summary.

II. KEY ENABLERS FOR LONG-HAUL FMF TRANSMISSION

Figure 1 shows the SDM transmission results we obtained employing FMF/MC-FMFs. The record-long transmission results presented in this paper were achieved mainly by combin-

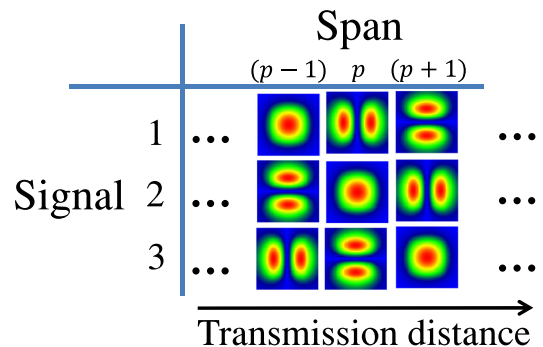


Fig. 2. Diagram of CMP transmission strategy for a 3-mode fiber.

ing transmission and signal processing techniques. This section aims to provide the details of those techniques.

A. Transmission With Cyclic Mode Permutation

It is a well-known fact that multimode fiber (MMF) was the first fiber deployed in the early stage of fiber-optic communication systems in the 1970s due to its larger spatial aperture property than that of single-mode fiber (SMF). Accordingly the physical characteristics of signal pulse evolution along a MMF were intensively studied in that period in terms of DMD and modal bandwidth. In particular, it was reported that the width of signal impulse responses exhibited the square root growth with fiber length, if multiple random modal coupling exists among its guided modes [25]–[28]. This can be understood from an analogy of dispersion between two polarization mode (i.e., polarization mode dispersion) in a SMF. A *coupled* transmission with random modal mixing is beneficial in terms of the computational complexity required for MIMO signal processing [29]. Unfortunately, modal coupling efficiency in a FM transmission fiber is expected to be low, since each modal group has highly unequal propagation constants – this is referred to as a weakly-coupled regime [10]. One effective way to deal with this is to introduce deliberately strong mode coupling along or between FMFs. Currently reported techniques to generate a strong coupling process include mode interchange using a mode multiplexer/demultiplexer pair [18], [19] or long-period fiber grating [20]–[22]. Even in uncoupled SDM transmission over MC fibers, a transmission scheme with a core-to-core signal rotation was found to bring the equalization effect for transmission performance over all cores [30], which generally represent different characteristics due to loss, dispersion, and inter-core crosstalk. In this paper, with the aim of achieving DMD-unmanaged long-haul FMF transmission, we propose a novel transmission scheme named CMP that provides significant suppression effects against DMD-induced pulse broadening. A schematic of CMP strategy is illustrated in Fig. 2. In transmission with CMP, each mode signal (including degenerate modes) is transformed into other mode signals before entering the next span via a mode-selective multiplexer/demultiplexer pair (for example, signals propagated as LP_{01} mode at the p -th span are converted and transmitted as LP_{11a} mode at the $(p + 1)$ -th span). Similarly, deliberate mode transformation is cyclically performed every span. Therefore, after information symbols are transmitted over several spans they are expected to periodically

path through each spatial channel in a cyclic manner. This equivalently achieves a quasi-strongly-coupled FMF transmission that suppresses pulse spreading and equalizes transmission performance. This will be shown in detail in Section IV.

B. Unreplicated Successive Interference Canceller

In optical MIMO systems, MIMO signal processing has a crucial role in detecting data streams from mutually-coupled received signals, even in weakly-coupled FMF transmission lines. One of the most popular signal processing method used in optical MIMO transmission is adaptive MIMO equalization using coefficient updating based on a stochastic gradient descent approach due to its properties of manageable complexity and channel tracking. Indeed, it has contributed to recently-achieved transmission reach extension [6], [9], [24]. In the presence of large MDL (and in a low signal-to-noise ratio (SNR) regime), however, intense residual intermodal crosstalk remaining after linear MIMO equalization for MDL-impaired MDM signals directly degrades post-processing signal-to-interference-noise ratio (SINR). The degradation is more severe in a higher MDL link due to stronger residual intermodal interference.

The scheme in which interference nulling and cancelling are performed sequentially, which is called successive interference cancellation (SIC) [31], is beneficial to improve SINR. We have proposed an unreplicated SIC (USIC) detection scheme to enhance tolerance against MDL that does not require computation of channel estimation for replica signal generation [23]. Conducted experiment results showed that the proposed USIC scheme outperformed the widely-used linear MIMO equalization and provided MDL tolerance improvement of 3.3 dB and OSNR gain of >4.5 dB. In the presented work we further modified the USIC scheme to employ soft estimates of transmitted symbols for interference subtraction, and applied it to MDL-impaired MDM signals propagating over long-haul FMF/MC-FMF transmission lines. The rest of this section is devoted to a description of the USIC-based detection scheme.

We consider an optical MIMO system with N_T transmitters and N_R receivers, and respectively define \mathbf{x} , \mathbf{y} , \mathbf{n} , and \mathbf{H} as $N_T \times 1$ transmitted signal vector, $N_R \times 1$ received vector, $N_R \times 1$ zero-mean complex Gaussian noise vector, and $N_R \times N_T$ channel transfer matrix. Each signal bit stream is independently coded at a transmitter, thus each symbol of the i -th symbol stream x_i with alphabet \mathcal{X} of cardinality size $|\mathcal{X}|$ carries coded bits $b_i \in \{0, 1\}$. MDM signal propagation in the optical MIMO system is modeled in a single equation:

$$\mathbf{y} = \mathbf{H}\mathbf{x} + \mathbf{n}. \quad (1)$$

At the receiver end, USIC detector is used for a signal detection purpose. It has a layered structure comprising multiple detection stages (Fig. 3), each of which is responsible for extracting a single data stream from received signals. Description of a deinterleaver is omitted in the presented work for brevity. In the initial stage, the k_1 -th data stream x_{k_1} is detected by a multiple-input single-output (MISO) detector without interference cancellation as

$$\hat{x}_{k_1} = \mathbf{w}_{(1)}^T \mathbf{y}_{(1)}, \quad (2)$$

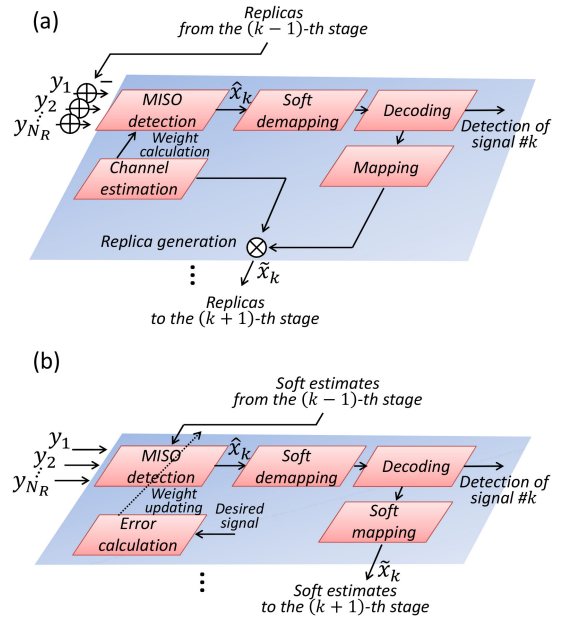


Fig. 3. Schematic of the k -th detection stage of (a) SIC detector and (b) USIC detector.

where $\mathbf{w}_{(k)}$, T , and \mathbf{y} are respectively MISO equalizer coefficient vector used at the k -th detection stage, the transpose operation, and $\mathbf{y}_{(1)} \stackrel{\text{def}}{=} [y_1 \ y_2 \ \dots \ y_{N_R}]^T$. Note that the subscript number in parenthesis for each quantity represents the USIC detection stage number. Then the soft demapper calculates the a posteriori log-likelihood ratio (LLR) values L_p^{dem} of the k_1 -th data stream by

$$L_p^{\text{dem}}[b_{k_1}(t_m)] \stackrel{\text{def}}{=} \ln \frac{p(\hat{x}_{k_1} | b_{k_1}(t_m) = 0)}{p(\hat{x}_{k_1} | b_{k_1}(t_m) = 1)}, \quad (3)$$

where $b_{k_1}(t_m)$ denotes m -th constituent bit of a t -th symbol in a k_1 -th signal stream ($m \in \{0, 1, \dots, \log_2 |\mathcal{X}| - 1\}$). Although L_p^{dem} in (3) is normally computed via Bayes' rule [32], iterative soft information exchange between a demapper and a decoder is not considered (i.e., no extrinsic LLR delivery) in the presented work for purposes of simplicity and low computational complexity. This corresponds to setting a priori LLR $L_a(b_{k_1}(t_m)) = \ln(P(b_{k_1}(t_m) = 0))/P(b_{k_1}(t_m) = 1)$ to zero. Thus (3) is simplified with the detection error variance σ^2 :

$$\begin{aligned} L_p^{\text{dem}}[b_{k_1}(t_m)] &= \ln \frac{p(b_{k_1}(t_m) = 0 | \hat{x}_{k_1})}{p(b_{k_1}(t_m) = 1 | \hat{x}_{k_1})} \\ &= \ln \frac{\sum_{x \in \mathcal{X}_m^0} \exp \left[-\frac{1}{2\sigma^2} \|\hat{x}_{k_1} - x\|^2 \right]}{\sum_{x \in \mathcal{X}_m^1} \exp \left[-\frac{1}{2\sigma^2} \|\hat{x}_{k_1} - x\|^2 \right]}, \end{aligned} \quad (4)$$

where \mathcal{X}_m^0 and \mathcal{X}_m^1 are symbol subsets defined as $\mathcal{X}_m^0 \stackrel{\text{def}}{=} \{x \in \mathcal{X} : b_m = 0\}$ and $\mathcal{X}_m^1 \stackrel{\text{def}}{=} \{x \in \mathcal{X} : b_m = 1\}$. Using redundancy information of a given error correction code, the channel decoder updates each bit reliability by using L_p^{dem} , and generates an a posteriori LLR sequence L_p^{dec} . Then using obtained L_p^{dec} , the probability for $b_{k_1}(t_m)$ is readily reconstructed as [33]

$$P[b_{k_1}(t_m)] = \frac{1}{1 + e^{-L_p^{\text{dec}}[b_{k_1}(t_m)]}} \cdot e^{-b_{k_1}(t_m) L_p^{\text{dec}}[b_{k_1}(t_m)]}. \quad (5)$$

On the basis of the probability calculation performed in (5), soft estimates of the t -th symbol in the k_1 -th data stream $\tilde{x}_{k_1}(t)$ are obtained as the expected value of the possible transmitted symbols averaged over all $x \in \mathcal{X}$:

$$\tilde{x}_{k_1}(t) = \sum_{x \in \mathcal{X}} x \prod_m P(b_{k_1}(t_m)). \quad (6)$$

Utilizing the soft estimates obtained in the first detection stage, the second stage starts signal detection through the MISO detector. We emphasize that, for interference elimination purposes, our USIC approach uses soft estimates not of the received data streams (i.e., replica signals) but of the transmitted data streams. This can be accomplished by directly feeding \tilde{x}_{k_1} into the MISO detector at the second stage as the $(N_R + 1)$ -th received signal. Accordingly, the *augmented* received signal vector used in the second stage $\mathbf{y}_{(2)}$ is obtained by

$$\mathbf{y}_{(2)} \stackrel{\text{def}}{=} \begin{bmatrix} \mathbf{y} \\ \tilde{x}_{k_1} \end{bmatrix}. \quad (7)$$

The equalizer coefficient vector used in the second stage $\mathbf{w}_{(2)}$ has $N_R + 1$ weight coefficients, where N_R is used for interference nulling, and 1 is used for interference canceling. The succeeding detection procedure of the detection stages is almost identical to that of the first stage, namely interference nulling and subtraction by a MISO detector (2), LLR computation by a soft demapper (4) and a channel decoder, soft estimate construction (6), and a received signal augmentation (7). The MISO detector at the k -th detection stage is allowed to utilize $(k - 1)$ soft estimates of the transmitted signals for interference elimination. This means that signal detection with higher reliability is achieved in the later stages.

It is worth noting describe how to obtain $\mathbf{w}_{(k)}$. If we define a detection error at the k -th stage for the i -th signal stream detection as $e_{(k)} = \hat{x}_i - x_i$, we can design $\mathbf{w}_{(k)}$ to minimize $\|e_{(k)}\|^2$ on the basis of the minimum mean squared error (MMSE) criterion:

$$\begin{aligned} \mathbf{w}_{\text{MMSE},(k)} &= \arg \min \mathbf{E} [\|e_{(k)}\|^2] \\ &= \arg \min_{\mathbf{w} \in \mathbb{C}^{(N_R+k-1) \times 1}} \mathbf{E} [\|\mathbf{w}_{(k)}^T \mathbf{y}_{(k)} - x_i\|^2], \end{aligned} \quad (8)$$

where $\mathbf{E}[\cdot]$ denotes the expectation operation. The widely-used practical strategy to recursively approach $\mathbf{w}_{\text{MMSE},(k)}$ is the least mean square (LMS) algorithm that evaluates an instantaneous estimate of the steepest gradient of the cost function by differentiating (8) with respect to $\mathbf{w}_{(k)}$. Thus we have an updating equation for $\mathbf{w}_{(k)}$ of

$$\mathbf{w}_{(k)} \leftarrow \mathbf{w}_{(k)} + \mu e_{(k)} \mathbf{y}_{(k)}^*, \quad (9)$$

where μ and $*$ denote respectively the step-size parameter and complex conjugate operation. Unlike the conventional SIC scheme, the overall processing of the USIC scheme presented in this paper contains no complex computation including the matrix inversion that is associated with channel estimation and replica signal generation.

Another important feature is the required computational complexity of the USIC scheme. The complexity can be estimated by a number of complex multiplications required in calculations

in (2) and (9) for all signal streams; the complexity required for decoding is not taken into account for complexity comparison between MIMO equalization and the USIC scheme, because decoding processing for each coded bit/block shall be performed only once for both schemes. If we consider a fully-loaded optical MIMO system (i.e., $N_T = N_R$) and let N be the number of transmitted signal streams, it can be easily shown that both detection schemes have the identical complexity order of $O(N^2)$ [24]. Although the above description of the USIC scheme is a time-domain representation, it is easily adaptable for processing in the frequency domain, as performed in our previous work [24].

III. EXPERIMENTAL SETUP

The experimental setup is illustrated in Fig. 4. At the transmitter, a test channel and nine additional channels were respectively generated by a tunable external-cavity laser (ECL) and distributed feedback (DFB) lasers located in the wavelength range from 1556.365 nm to 1557.274 nm. The even/odd channels and the test channel, all having 12.5-GHz frequency spacing, were produced by independent signal patterns, IQ modulators, and polarization division multiplexing (PDM) emulators with a 100-ns delay. The transmission frame of 33040 symbol-length contained 2.9%-overhead (OH) for the training sequence and a 32400-symbol-length pattern produced by a low-density parity-check (LDPC) code with the 4/5 code rate defined in the digital video broadcasting-satellite second generation (DVB-S2) [34] standard, which is devoted to the accurate soft estimate construction used for interference cancelling in USIC signal detection. We also assumed a 7%-OH hard-decision (HD) outer forward error correction (FEC) code comprising the Reed-Solomon code of RS(1023, 1007) and the Bose-Chaudhuri-Hocquenghem code of BCH(2047, 1952) defined in ITU-T Recommendation G.975.1. We adopted a parallel MIMO transmission technique [24] in which dual subcarriers driven at 6 Gbaud were digitally generated. This yielded 10-WDM 12.5-GHz spaced 48 Gb/s QPSK signals, resulting in spectral efficiency (SE) of 2.79 b/s/Hz/mode/core. Then all optical carriers were combined through interleave filters and couplers, and then split and delayed with 206 ns for the LP_{11a} input and 439 ns for the LP_{11b} input. We labeled each signal stream as modes 1, 2, and 3, which were respectively transmitted as LP₀₁, LP_{11a}, and LP_{11b} at the initial span. We constructed a recirculating loop system and used it for the test channel measurement. It comprised a graded-index (GI) FMF/MC-FMF designed to have a low DMD, a physical-contact type fan-in/fan-out (FI/FO) devices, low-loss mode-selective mode multiplexer/demultiplexer based on index matching by asymmetric mode couplers, single-mode erbium-doped amplifiers (EDFAs), Raman-pump combiners, variable optical attenuators (VOAs), loop-synchronous polarization scramblers, and acousto-optic modulators (AOMs). We evaluated the transmission performance obtained with single-core 3-mode and 12-core \times 3-mode MC FM transmission fibers [35]. A 75.2-km FMF transmission line was constructed by fusion splicing three spools. The 52.7-km MC-FMF transmission line has twelve cores with heterogeneous trench-assisted GI profiles placed in

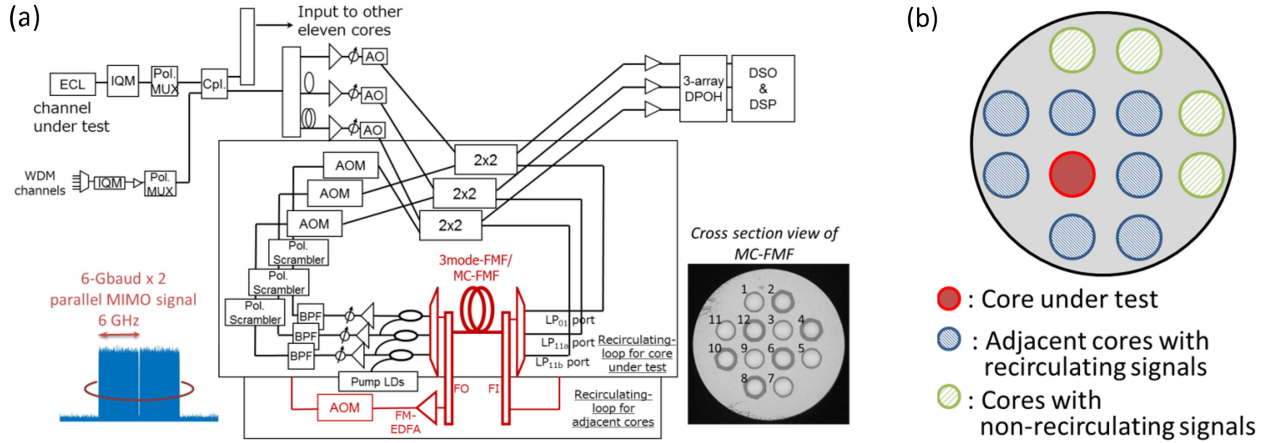


Fig. 4. (a) Experimental setup. (b) Signal loading map into MC-FMF.

a square lattice arrangement. For both fibers, each core had a DMD of <0.1 ns/km, and an effective area (A_{eff}) of $>111 \mu\text{m}^2$ for LP_{01} . The core #6 represented the largest DMD, while the highest MDL was observed in core #4. The worst inter-core crosstalk at 1550 nm arising in the MC-FMF including the FI/FO devices was so small (i.e., -48.4 dB after 500-km transmission [24]) that its impact on signal performance was negligible in the presented work. The CMP scheme was introduced in a way such that the AOM output ports of each recirculating loop were mutually switched, and connected to other recirculating loop input ports. Note that the impact of inserting a mode demultiplexer on increased loss and MDL was mitigated by the use of the distributed Raman amplification. To load transmission signals into all MC-FMF cores, we constructed seven other recirculating loop systems for adjacent cores with a core-to-core delay of more than 600 ns, in which MDM signals were amplified by low-MDL ring-core FM-EDFAs [36]. We also constructed four non-recirculating systems for signal loading into the remaining four cores. At the receiver end, the transmitted signals were digitized, stored, and processed by 6×6 MIMO processing. Dual subcarriers were processed in a parallel manner to remove distortions arising from DMD and MDL effects. After bit error rates (BERs) were counted using 0.26 Mbits per spatial channel, Q-factors were obtained for both before and after LDPC decoding. Note that our detection method included determining whether or not to conduct USIC-based detection. In particular, when Q-factors without USIC detection were below 5 dB, we applied the USIC detection technique; otherwise MDM signals were detected by employing the conventional linear MIMO equalization. In the USIC processing, signal detection started from mode 1, followed by modes 2 and 3. A more detailed processing description was given in Section II. After signal detection, LDPC-decoded binary sequences were obtained by using the sum-product algorithm with soft-decision decoding in the logarithm domain.

IV. TRANSMISSION RESULTS

Prior to the transmission experiments, we explored the performance improvement achieved by the proposed CMP and

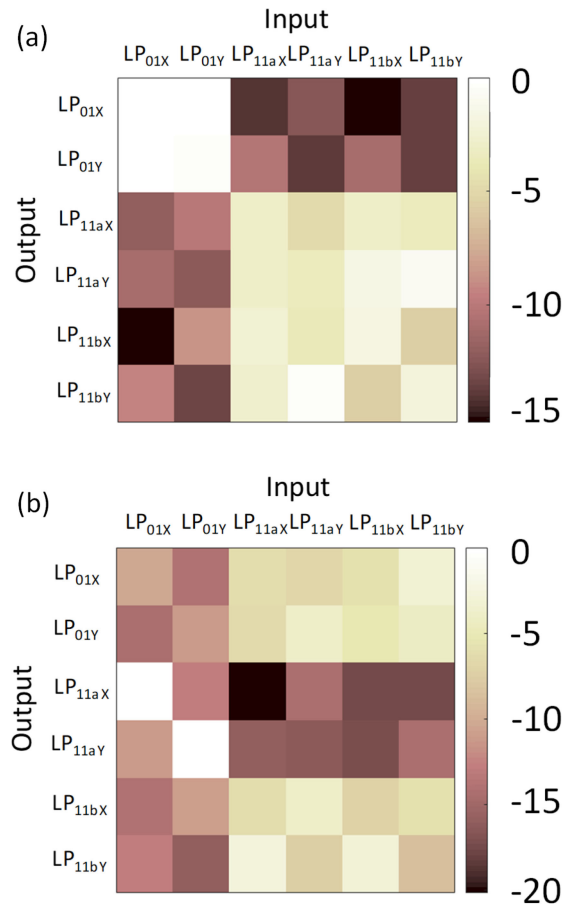


Fig. 5. Crosstalk matrix at the initial span output for signals of λ_S transmitted over core #12 of the MC-FMF in dB unit (a) without the CMP scheme and (b) with the CMP scheme.

USIC schemes. Then the main transmission results are presented where the WDM SDM signals were transmitted over a 3-mode FMFs having single-core or 12-core with the transmission reach exceeding a thousands of km.

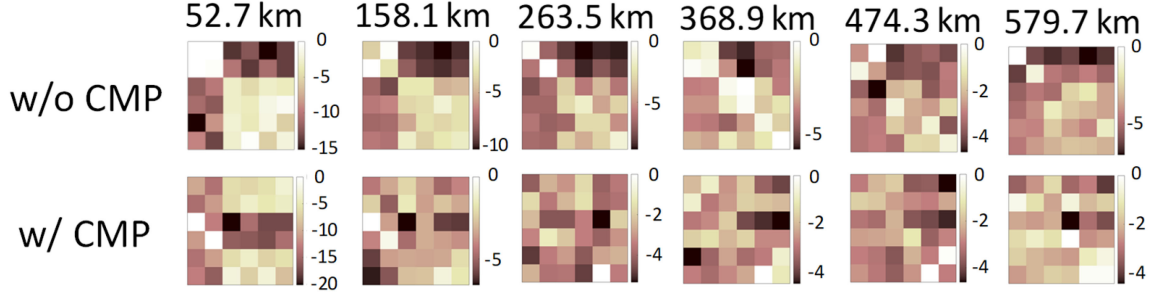


Fig. 6. Crosstalk matrix transition for signals of λ_5 transmitted over core #12 of the MC-FMF with increased transmission distance. Each panel is represented in the same figure format as in Fig. 5.

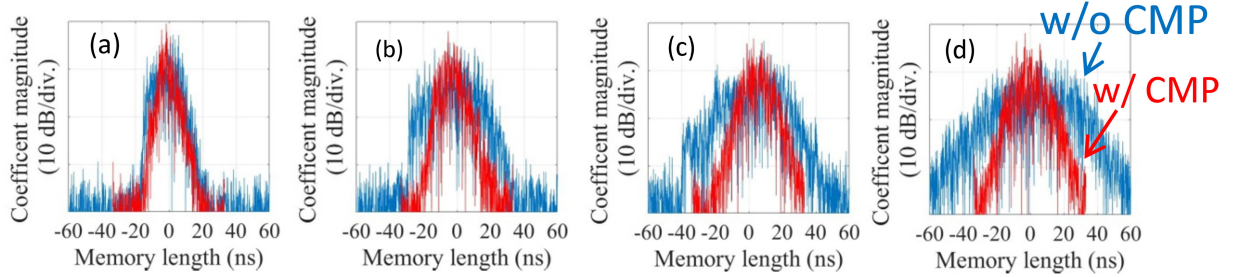


Fig. 7. Memory length expansion for signals of λ_5 transmitted over core #6 of the MC-FMF. (a) 527 km, (b) 1054 km, (c) 1581 km, and (d) 2108 km.

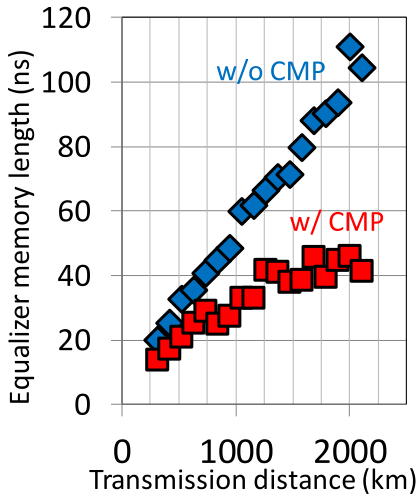


Fig. 8. Memory length growth as a function of transmission distance for signals of λ_5 transmitted over core #6 of the MC-FMF.

A. DMD and MDL Impact Mitigation by the CMP Scheme

To examine the benefits in the transmission with the CMP scheme, we performed experiments on LMS-based channel estimation of \mathbf{H} both with and without the CMP scheme. Through analysis of the obtained \mathbf{H} , we calculated the input power coupling into each output mode, which is correspondingly shown as a crosstalk matrix between spatial modes (including polarization modes). Fig. 5 compares the modal crosstalk matrix with and without the CMP scheme at the initial span output for core #12 of the MC-FMF. For the conventional FMF transmission (i.e., without the CMP scheme), little power exchange between mode groups was observed; this corresponds to a weakly-coupled transmission regime. However, when we applied the

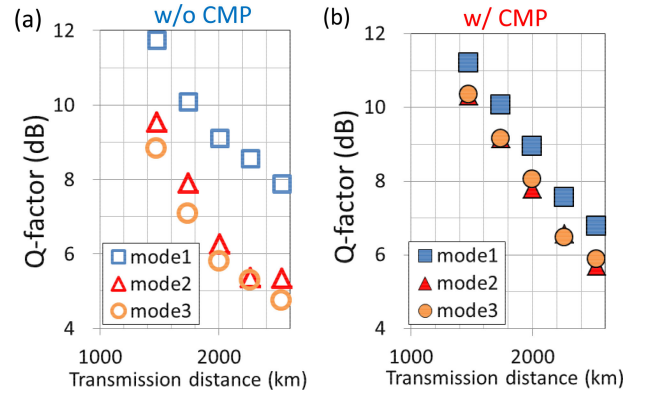


Fig. 9. Q-factor comparison obtained by MIMO equalization for signals of λ_5 transmitted over core #4 in an MC-FMF (a) without and (b) with the CMP scheme.

CMP scheme, the relation between input/output ports markedly changed. We consider that introducing the CMP scheme converts \mathbf{H} to \mathbf{H}_{CMP} . This process is substantially modeled as

$$\mathbf{H}_{\text{CMP}} \stackrel{\text{def}}{=} \mathbf{P}\mathbf{H}, \quad (10)$$

where we used the permutation matrix \mathbf{P} , defined as

$$\mathbf{P} \stackrel{\text{def}}{=} \begin{pmatrix} 0 & 0 & 0 & 0 & 1 & 0 \\ 0 & 0 & 0 & 0 & 0 & 1 \\ 1 & 0 & 0 & 0 & 0 & 0 \\ 0 & 1 & 0 & 0 & 0 & 0 \\ 0 & 0 & 1 & 0 & 0 & 0 \\ 0 & 0 & 0 & 1 & 0 & 0 \end{pmatrix}. \quad (11)$$

Note that in (11), the crosstalk in the non-diagonal entries induced in practical mode multiplexers/demultiplexers is ignored for simplicity. We further calculated the crosstalk matrix for

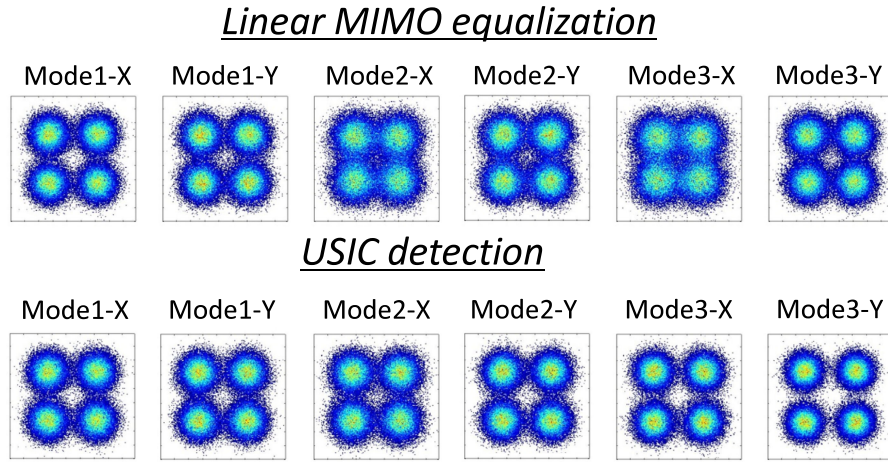


Fig. 10. Signal constellation comparison between conventional linear equalization (top) and USIC detection (bottom) for signals of λ_5 after 2500-km transmission over core #4 of an MC-FMF.

both cases at longer transmission distances, and summarized the results in Fig. 6. Without the CMP scheme the coupling efficiency between different mode group was kept low (e.g., < -5 dB) at distances up to 500 km. However, transmission with the scheme yielded a highly-mixed crosstalk matrix even after transmission over several spans. This confirms that using the scheme effectively stimulates the power coupling process; we called this *quasi-strongly-coupled transmission*.

Figures 7(a) through (d) represent the DMD-induced EML broadening observed in core #6 of an MC-FMF. They clearly show that the CMP strategy significantly suppressed EML within almost ± 20 ns even after 2000-km transmission. Fig. 8 shows the evolution of EML as a function of transmission distance. While EMLs scaled almost linearly with an increased transmission distance in conventional weakly-coupled transmission, the CMP transmission introduced a squared-root growth of EMLs, which is generally observed in strongly-coupled transmission fibers. The EML suppression effect achieved by the CMP corresponds to more than a 50% decrease in the required EML after 2500-km transmission over an MC-FMF. In addition, the CMP provides suppression effects against MDL as well as DMD. Fig. 9 compares the obtained Q-factors for both transmission setups over core #4 of an MC-FMF. In the conventional transmission, the signals propagated mainly as higher-order spatial modes (i.e., LP_{11}) degraded severely relative to those of the fundamental mode. In contrast, the mode-to-mode Q-factor gap was well suppressed in the CMP transmission. This implies that the CMP effectively mitigated the MDL impact by permutating each mode signal in every span.

B. MDL-Induced Interference Cancellation by the USIC Detection

Next, we show the USIC detection performance in the presence of a large MDL. Fig. 10 compares the signal constellations obtained with conventional linear MIMO equalization (top) and USIC detection (bottom) for the signals after 2500-km propagation over core #4 of an MC-FMF. While the

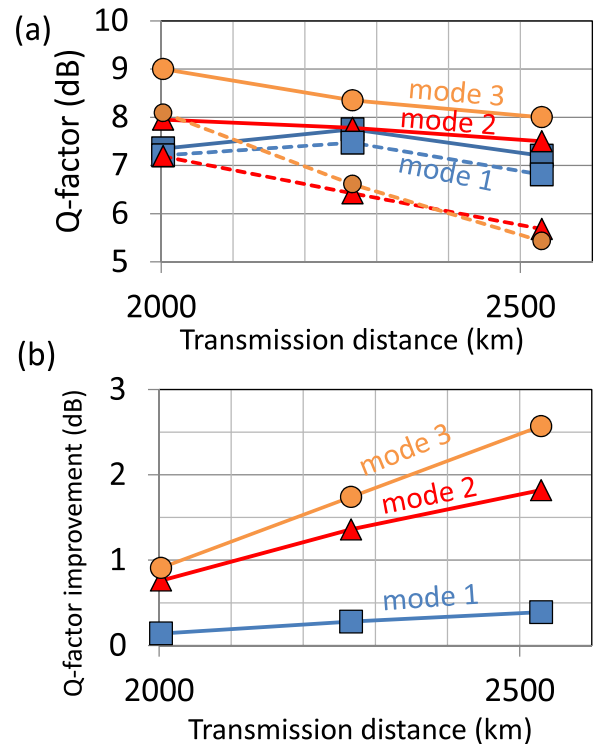


Fig. 11. (a) Q-factors obtained by MIMO equalization (broken lines) and USIC detection (solid lines) for signals of λ_5 in core #4. (b) Q-factor improvements achieved by USIC detection with respect to MIMO equalization.

spatial channels for modes 2 and 3 were contaminated by the MDL-induced intermodal crosstalk in the MIMO equalization case, the detection based on the USIC scheme effectively removed those interference signals and hence provided superior detection performance. Then USIC detection performance is quantitatively evaluated with Q-factor comparison in Fig. 11(a) and Q-factor improvement in Fig. 11(b). Q-factor improvement was defined as the Q-factor difference between those obtained by MIMO equalization and USIC detection. Higher Q-factor gains were obtained in the later stages of USIC detection

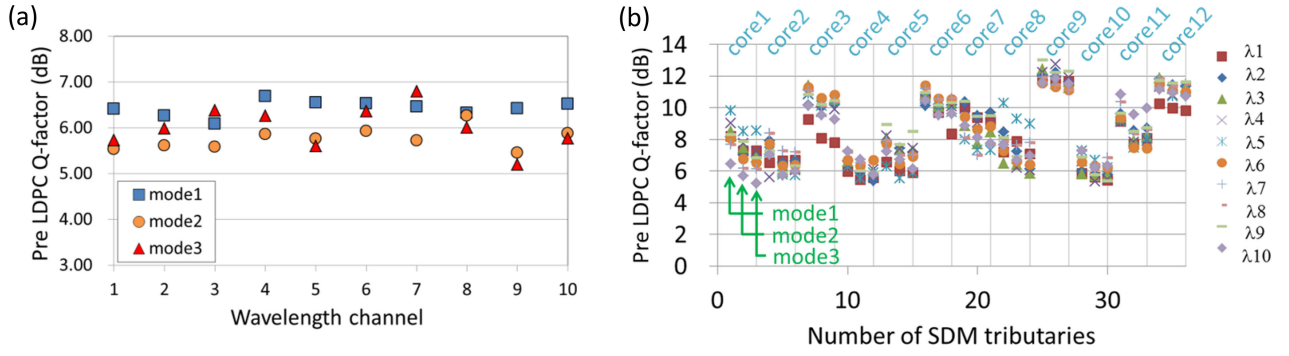


Fig. 12. Q-factors obtained by MIMO equalization or theUSIC detection after transmission over (a) 6316.8-km FMF and (b) 2529.6-km MC-FMF for all measured channels.

because larger numbers of decoded signal streams were used for interference cancellation. For 2500-km transmission, Q-factors improved by more than 2 dB for signals of mode 3.

C. Transmission Performance

Finally, we evaluated the Q-factors obtained after transmission over 6316.8-km (84 loops) FMF and 2529.6-km (48 loops) MC-FMF. Fig. 12 summarizes the obtained Q-factors before LDPC decoding for the transmissions over FMF (Fig. 12(a)) and MC-FMF (Fig. 12(b)), respectively. In MC-FMF transmission, better signal performance was obtained for the inner cores (#3, #6, #9, and #12) than that for the outer cores (#1, #2, #4, #5, #7, #8, #10, and #11). We consider that the core-to-core signal performance difference was mainly originated from larger MDL for the outer cores due to the rotational misalignment at the FI/FO devices [37]. We confirmed that all the measured pre-LDPC Q-factors exceeded 5.0 dB, and that the post-LDPC Q-factors became higher than the 9.1-dB Q-limit of the 7%-OH HD-FEC.

V. CONCLUSION

We have successfully demonstrated differential mode delay (DMD)-unmanaged space division multiplexing (SDM) transmission over a record transmission reach of 2500 km for a 36-SDM (12-core \times 3-mode) multicore fewmode fiber (MC-FMF) and 6300 km for a 3-mode FMF. This was achieved by two novel key techniques that significantly enhance the transmission performance of mode division multiplexed (MDM) signals in the presence of DMD and mode dependent loss (MDL). The first is a cyclic mode permutation (CMP) transmission scheme that greatly reduces DMD and MDL impacts by converting weakly-coupled MC-FMF/FMF transmission lines into quasi-strongly-coupled transmission lines. Second is an unreplicated successive interference cancelling (USIC) technique that effectively eliminates intermodal interference arising from the residual MDL and enables Q-factor improvement exceeding 2 dB. Combining the use of these techniques is a promising way to achieve long-haul SDM systems using FMFs as transmission media.

ACKNOWLEDGMENT

Part of this research utilized results from research commissioned by the National Institute of Information and Communications Technology (NICT) of Japan.

REFERENCES

- [1] T. Morioka, "New generation optical infrastructure technologies: 'EXAT initiative' towards 2020 and beyond," in *Proc. 14th OptoElectronics Commun. Conf.*, Hong Kong, China, Jul. 2009, Paper FT4.
- [2] H. Takara *et al.*, "1.01-Pb/s (12 SDM/222 WDM/456 Gb/s) crosstalk-managed transmission with 91.4-b/s/Hz aggregate spectral efficiency," in *Proc. 38th Eur. Conf. Exhib. Opt. Commun.*, Amsterdam, The Netherlands, Sep. 2012, Paper Th.3.C.1.
- [3] B. J. Puttnam *et al.*, "2.15 Pb/s transmission using a 22 core homogeneous single-mode multi-core fiber and wideband optical comb," in *Proc. 41st Eur. Conf. Opt. Commun.*, Valencia, Spain, Sep. 2015, Paper PDP.3.1.
- [4] D. Soma *et al.*, "10.16 Peta-bit/s dense SDM/WDM transmission over low-DMD 6-mode 19-core fibre across C + L band," in *Proc. 43rd Eur. Conf. Opt. Commun.*, Gothenburg, Sweden, Sep. 2017, Paper Th.PDP.A.1.
- [5] A. Turukhin *et al.*, "105.1 Tb/s power-efficient transmission over 14,350 km using a 12-core fiber," in *Proc. 39th Opt. Fiber Commun. Conf. Exhib.*, Anaheim, CA, USA, Mar. 2016, Paper Th4C.1.
- [6] J. van Weerdenburg *et al.*, "Mode-multiplexed 16-QAM transmission over 2400-km large-effective-area depressed-cladding 3-mode fiber," in *Proc. 43rd Opt. Fiber Commun. Conf. Exhib.*, San Diego, CA, USA, Mar. 2018, Paper W4C.2.
- [7] G. Rademacher *et al.*, "159 Tbit/s C + L band transmission over 1045 km 3-mode graded-index few-mode fiber," in *Proc. 43rd Opt. Fiber Commun. Conf. Exhib.*, San Diego, CA, USA, Mar. 2018, Paper Th4C.4.
- [8] K. Shibahara *et al.*, "DMD-unmanaged long-haul SDM transmission over 2500-km 12-core \times 3-mode MC-FMF and 6300-km 3-mode FMF employing intermodal interference cancelling technique," in *Proc. 43rd Opt. Fiber Commun. Conf. Exhib.*, San Diego, CA, USA, Mar. 2018, Paper Th4C.6.
- [9] G. Rademacher *et al.*, "3500-km mode-multiplexed transmission through a three-mode graded-index few-mode fiber link," in *Proc. 43rd Eur. Conf. Opt. Commun.*, Gothenburg, Sweden, Sep. 2017, Paper M.2.E.4.
- [10] J. M. Kahn, K.-P. Ho, and M. B. Shemirani, "Mode coupling effects in multi-mode fibers," in *Proc. 37th Opt. Fiber Commun. Conf. Exhib.*, Los Angeles, CA, USA, Mar. 2012, Paper OW3D.3.
- [11] A. Lobato *et al.*, "Impact of mode coupling on the mode-dependent loss tolerance in few-mode fiber transmission," *Opt. Express*, vol. 20, pp. 29776–29783, Dec. 2012.
- [12] D. Soma *et al.*, "2.05 Peta-bit/s super-Nyquist-WDM SDM transmission using 9.8-km 6-mode 19-core fiber in full C band," in *Proc. 41st Eur. Conf. Opt. Commun.*, Valencia, Spain, Sep. 2015, Paper PDP 3.2.
- [13] R. Ryf *et al.*, "10-mode mode-multiplexed transmission over 125-km single-span multimode fiber," in *Proc. 41st Eur. Conf. Opt. Commun.*, Valencia, Spain, Sep. 2015, Paper PDP 3.3.
- [14] N. K. Fontaine *et al.*, "30 \times 30 MIMO transmission over 15 spatial modes," in *Proc. 40th Opt. Fiber Commun. Conf. Exhib.*, Los Angeles, CA, USA, Mar. 2015, Paper Th5C.1.

- [15] R. Ryf *et al.*, "708-km combined WDM/SDM transmission over few-mode fiber supporting 12 spatial and polarization modes," in *Proc. 39th Eur. Conf. Exhib. Opt. Commun.*, London, U.K., Sep. 2013, Paper We.2.D.1.
- [16] V. Sleiffer *et al.*, "73.7 Tb/s ($96 \times 3 \times 256$ -Gb/s) mode-division-multiplexed DP-16QAM transmission with inline MM-EDFA," in *Proc. 38th Eur. Conf. Exhib. Opt. Commun.*, Opt. Soc. Amer., Amsterdam, The Netherlands, Sep. 2012, Paper Th.3.C.4.
- [17] R. Ryf *et al.*, "Space-division multiplexed transmission over 4200 km 3-core microstructured fiber," in *Proc. 37th Opt. Fiber Commun. Conf. Exhib.*, Los Angeles, CA, USA, Mar. 2012, Paper PDP5C.2.
- [18] S. O. Arik, K. P. Ho, and J. M. Kahn, "Group delay management and multiinput multioutput signal processing in mode-division multiplexing systems," *J. Lightw. Technol.*, vol. 34, no. 11, pp. 2867–2880, Jun. 2016.
- [19] Y. Wakayama, D. Soma, K. Igarashi, H. Taga, and T. Tsuritani, "Intermediate mode interchange for reduction of differential mode-group delay in weakly-coupled 6-mode fiber transmission line," in *Proc. 41th Opt. Fiber Commun. Conf. Exhib.*, Mar. 2016, Paper M3E.6.
- [20] J. Fang, A. Li, and W. Shieh, "Low-DMD few-mode fiber with distributed long-period grating," *Opt. Lett.*, vol. 40, no. 17, pp. 3937–3940, Sep. 2015.
- [21] H. Liu, H. Wen, R. Amezcua-Correa, P. Sillard, and G. Li, "Reducing group delay spread in a 9-LP mode FMF using uniform long-period gratings," in *Proc. 40th Opt. Fiber Commun. Conf. Exhib.*, Los Angeles, CA, USA, Mar. 2017, Paper Tu2J.5.
- [22] A. Hasegawa-Urushibara, T. Mori, T. Sakamoto, M. Wada, T. Yamamoto, and K. Nakajima, "Experimental verification of mode-dependent loss reduction by mode coupling using long-period grating," in *Proc. 40th Opt. Fiber Commun. Conf. Exhib.*, Los Angeles, CA, USA, Mar. 2017, Paper Tu2J.6.
- [23] K. Shibahara, T. Mizuno, and Y. Miyamoto, "LDPC-coded FMF transmission employing unreplicated successive interference cancellation for MDL-impact mitigation," in *Proc. 43rd Eur. Conf. Opt. Commun.*, Gothenburg, Sweden, Sep. 2017, Paper Th.1.D.4.
- [24] K. Shibahara *et al.*, "Dense SDM (12-core \times 3-mode) transmission over 527 km with 33.2-ns mode-dispersion employing low-complexity parallel MIMO frequency-domain equalization," *J. Lightw. Technol.*, vol. 34, no. 1, pp. 196–204, Jan. 2016.
- [25] S. D. Personick, "Time dispersion in dielectric waveguides," *Bell Syst. Tech. J.*, vol. 50, pp. 843–859, Mar. 1971.
- [26] R. Olshansky, "Mode coupling effects in graded-index optical fibers," *Appl. Opt.*, vol. 14, pp. 935–945, Apr. 1975.
- [27] L. G. Cohen and S. D. Personick, "Length dependence of pulse dispersion in a long multimode optical fiber," *Appl. Opt.*, vol. 14, pp. 1357–1360, Jun. 1975.
- [28] K. Kitayama, S. Seikai, and N. Uchida, "Impulse response prediction based on experimental mode coupling coefficient in a 10-km long graded-index fiber," *IEEE J. Quantum Electron.*, vol. 16, no. 3, pp. 356–362, Mar. 1980.
- [29] S. O. Arik, J. M. Kahn, and K. P. Ho, "MIMO signal processing for mode-division multiplexing: An overview of channel models and signal processing architectures," *IEEE Signal Process. Mag.*, vol. 31, no. 2, pp. 25–34, Mar. 2014.
- [30] S. Chandrasekhar *et al.*, "Wdm/sdm transmission of 10×128 -Gb/s PDM-QPSK over 2688-km 7-core fiber with a per-fiber net aggregate spectral-efficiency distance product of 40,320 km b/s/Hz," in *Proc. 37th Eur. Conf. Exhib. Opt. Commun. (ECOC 2011)*, Geneva, Switzerland, Sep. 2011, Paper Th.13.C.4.
- [31] P. W. Wolniansky, G. J. Foschini, G. Golden, and R. A. Valenzuela, "V-BLAST: An architecture for realizing very high data rates over the rich-scattering wireless channel," in *Proc. URSI Int. Symp. Signals, Syst., Electron.*, 1998, pp. 295–300.
- [32] S. ten Brink, J. Speidel, and R.-H. Yan, "Iterative demapping and decoding for multilevel modulation," in *Proc. IEEE GLOBECOM 1998 (Cat. NO.98CH36250)*, Sydney, NSW, Australia, Nov. 1998, vol. 1, pp. 579–584.
- [33] J. Hagenauer, "The EXIT chart-introduction to extrinsic information transfer in iterative processing," in *Proc. 12th Eur. Signal Process. Conf.*, 2004, pp. 1541–1548.
- [34] ETSI, "User guidelines for the second generation system for broadcasting, interactive services, news gathering and other broadband satellite applications (DVB-S2)," Eur. Telecommun. Standards Inst., Sophia Antipolis, France, Tech. Rep., 102376, Feb. 2015.
- [35] K. Saitoh and S. Matsuo, "Multicore fiber technology," *J. Lightw. Technol.*, vol. 34, no. 1, pp. 55–66, Jan. 2016.
- [36] H. Ono, T. Hosokawa, K. Ichii, S. Matsuo, and M. Yamada, "Improvement of differential modal gain in few-mode fibre amplifier by employing ring-core erbium-doped fibre," *Electron. Lett.*, vol. 51, no. 2, pp. 172–173, Jan. 2015.
- [37] T. Sakamoto *et al.*, "High spatial density six-mode seven-core fibre for repeated dense SDM transmission," in *Proc. 43rd Eur. Conf. Opt. Commun. (ECOC 2017)*, Gothenburg, Sweden, Sep. 2017, Paper Th.PDPA.6.

Kohki Shibahara (M'15) received the B.S. degree in physics, the M.S. degree in geophysics, and the Ph.D. degree in informatics from Kyoto University, Kyoto, Japan, in 2008, 2010, and 2017, respectively. He joined NTT Network Innovation Laboratories in 2010. His current research interests include spatial division multiplexing transmission systems and advanced multiple-input and multiple-output signal processing. He is a member of IEICE and the IEEE Photonics Society. He received the Tingye Li Innovation Prize from OSA in 2016 and the Young Researcher's Award from IEICE in 2017.

Takayuki Mizuno (M'04) received the B.E. degree in applied physics, the M.E. degree in crystalline materials science, and the Dr. Eng. degree in quantum engineering, all from Nagoya University, Nagoya, Japan, in 1998, 2000, and 2007, respectively.

In 2000, he joined the NTT Photonics Laboratories, NTT Corporation, Japan, where he was involved in the research and development of silica planar light-wave circuit optical waveguide devices, including arrayed-waveguide gratings, Mach-Zehnder interferometer-based filters and switches, and digital coherent demodulators for advanced modulation formats. Since 2013, he has been a Senior Research Engineer with the NTT Network Innovation Laboratories, NTT Corporation, Japan. His current research interests include space-division multiplexed transmission technology for ultrahigh-capacity optical transport systems.

He is a member of the IEEE Photonics Society, the Optical Society of America, and the Institute of Electronics, Information and Communication Engineers. He is currently serving in the technical program committee of the Optical Fiber Communication Conference.

Doohwan Lee received the B.S. (Hons.) and M.S. degrees in electrical engineering from Seoul National University, Seoul, South Korea, in 2004 and 2006, respectively, and the Ph.D. degree in electrical engineering and information systems from the University of Tokyo, Tokyo, Japan, in 2009. He has been with NTT Network Innovation Laboratories since 2009. From 2012 to 2014, he was an Assistant Professor with the Research Center for Advanced Science and Technology, University of Tokyo. Since 2016, he has been a part-time Lecturer with Kanagawa University, Yokohama, Japan. His research interests include compressed sensing, software/cognitive radio, signal processing, and OAM multiplexing. He received the Best Paper Award and Best Technical Exhibition Award from the IEICE Software Radio in 2011, the IEICE Communications Society Excellent Paper Award in 2012, the IEICE SRW (Short Range Wireless Communications) Young Researcher's Award in 2016, the Best Technical Exhibition Award from SmartCom 2014, the Best Paper Award from SmartCom 2016, and the Best Paper Award and Special Technical Award in Smart Radio from IEICE Smart Radio in 2017.

Yutaka Miyamoto (M'93) received the B.E. and M.E. degrees in electrical engineering from Waseda University, Tokyo, Japan, in 1986 and 1988, respectively, and the Dr. Eng. degree in electrical engineering from the University of Tokyo, Tokyo, Japan. In 1988, he joined NTT Transmission Systems Laboratories, where he engaged in R&D of high-speed optical communications systems including the first 10-Gb/s terrestrial optical transmission system (FA-10G) using EDFA (erbium-doped optical fiber amplifier) inline repeaters. From 1995 to 1997, he was with NTT Electronics Technology Corporation, where he worked on the planning and product development of high-speed optical modules at data rates of 10 Gb/s and beyond. Since 1997, he has been with NTT Network Innovation Labs, where he has been researching and developing optical transport technologies based on 40/100/400-Gb/s channels and beyond. He has also been investigating and promoting a scalable optical transport network with Pb/s-class capacity based on innovative transport technologies such as digital signal processing, space division multiplexing, and cutting-edge integrated devices for photonic preprocessing. He is currently the Chair of the IEICE technical committee of Extremely Advanced Optical Transmission. He is a Fellow of IEICE.

Hirofumi Ono (M'96–SM'15) received the B.S., M.S., and Ph.D. degrees in applied physics from Tohoku University, Sendai, Japan, in 1993, 1995, and 2004, respectively. He joined the NTT Laboratories, Tokai, Japan, in 1995. He was also a Visiting Research Fellow with the Optoelectronics Research Centre, University of Southampton, Southampton, U.K., from 2005 to 2006. He has been involved in research on optical fiber amplifiers, including L- and S-band erbium-doped fiber amplifiers. He has also undertaken research on highly nonlinear fiber devices, photonic crystal fibers, and wavelength-division multiplexing transmission systems. His current research interests include fiber and waveguide devices, including optical amplifiers, used for space-division multiplexing systems. He is a member of the Institute of Electronic, Information and Communication Engineers of Japan and the Japan Society of Applied Physics.

Kazuhide Nakajima (M'05) received M.S. and Ph.D. degrees in electrical engineering from Nihon University, Chiba, Japan, in 1994 and 2005, respectively. In 1994, he joined NTT Access Network Systems Laboratories, Tokai, Japan, where he engaged in research on optical fiber design and related measurement techniques. He is currently a Group Leader (Senior Distinguished Researcher) of NTT Access Network Service Systems Laboratories. He has been acting as a Rapporteur of Q5/SG15 of ITU-T since 2009. He is a member of the Optical Society of America, the Institute of Electronics, Information and Communication Engineers of Japan, and the Japan Society of Applied Physics.

Yoshimichi Amma received the B.S. and M.S. degrees in mechanical engineering from Yokohama National University, Kanagawa, Japan, in 2010 and 2012, respectively.

He joined the Optical Fibre Technology Department, Optics and Electronics Laboratory, Fujikura, Ltd., Chiba, Japan, in 2012. He has six years of experience in research and development of multicore fibers. He is a member of the Institute of Electronics, Information and Communication Engineers of Japan.

Katsuhiko Takenaga received the B.S. degree from Shinshu University, Nagano, Japan, and the M.S. degree from Hokkaido University, Sapporo, Japan, in 1999 and 2001, both in physics.

In 2001, he joined Fujikura, Ltd., Chiba, Japan, where he has been involved in research and development of optical fibers. He is a member of the Institute of Electronics, Information and Communication Engineers of Japan.

Kunimasa Saitoh (S'00–M'01) received the B.S., M.S., and Ph.D. degrees in electronic engineering from Hokkaido University, Sapporo, Japan, in 1997, 1999, and 2001, respectively. From 1999 to 2001, he was a Research Fellow of the Japan Society for the Promotion of Science. From 2001 to 2005, he was a Research Associate with the Graduate School of Engineering, Hokkaido University. From 2005 to 2013, he was an Associate Professor with the Graduate School of Information Science and Technology, Hokkaido University, where he became a Professor in 2013. He has been involved in research on fiber optics, nano-photonics, integrated optical devices, and computer-aided design and modeling of guided-wave devices. He is the author of more than 200 research papers in refereed international journals and more than 250 refereed international conference presentations. He is a member of the Optical Society of America and the Institute of Electronics, Information and Communication Engineers (IEICE). He was a Chair of Subcommittee D4 of Optical Fiber Communication Conference in 2016. He is currently on the Technical Program Committee of European Conference on Optical Communication. He received the Excellent Paper Award and the Young Scientist Award from the IEICE in 1999 and 2002, respectively, the Young Scientists Prize of the Commendation for Science and Technology from the Ministry of Education, Culture, Sports, Science, and Technology, Government of Japan, in 2008, the JSPS Prize from the Japan Society for the Promotion of Science in 2015, and the Distinguished Lecturers Award from the IEEE Photonics Society in 2017.